# APPLICATIONS OF KHZ-CW LIDAR IN ECOLOGICAL ENTOMOLOGY

**Conference Paper** · June 2015

CITATIONS
0

READS
126

**2 authors:**

Elin Malmqvist
Lund University
**7** PUBLICATIONS **1** CITATION
SEE PROFILE

Mikkel Brydegaard
Lund University
**54** PUBLICATIONS **246** CITATIONS
SEE PROFILE

# APPLICATIONS OF KHZ-CW LIDAR IN ECOLOGICAL ENTOMOLOGY

**Elin Malmqvist [1,2]*, Mikkel Brydegaard[1,2]**

*[1]Lunds Laser Centre (LLC), Lund University, Lund, Sweden, *Email: elin.malmqvist@forbrf.lth.se*

*[2]Centre of Animal Movement Research (CAnMove), Lund University, Sweden*

## ABSTRACT

The benefits of kHz lidar in ecological entomology is explained. Results from kHz-measurements on insects, carried out with a CW-lidar system, employing the Scheimpflug principle to obtain range resolution, are presented. A method to extract insect events and analyze the large amount of lidar data is also described.

## 1. INTRODUCTION

Insects are a very dominant group of animals on Earth and they are essential in most ecosystems. The ability to systematically and efficiently detect, identify and monitor insects is of great interest from an ecological, as well as an economic and social, point of view. For instance, pollinators and insect pests have great impact on agriculture, and therefore also on food production. Many insects, such as malaria mosquitos, also function as disease vectors [1].

Over the last several decades, lidar methods have been used and developed for different varieties of atmospheric monitoring, see e.g. [2]. Our research group at Lund University have in recent years explored opportunities for applications in ecological entomology [3]. Lidar measurements can provide continuous and extensive monitoring of insects, which is impossible for manual methods such as collection in sweep nets or traps. Information about insect properties such as size, velocity and wing beat frequency can be extracted from lidar data. These properties span a parameter space with a certain dimensionality. A higher dimensionally of this space increases the likelihood of successful separation between different species, sexes and age groups.

Due to their natural wing beat cycle, flying insects are seen as blinking scattering particles, meaning that the backscattered lidar signal, defined in terms of an optical cross section (OCS) with unit $cm^2$, is modulated. The fundamental frequency of insect wing beats can vary between 10-1000 Hz [4], and we have seen that the signal can contain up to 20 harmonics due to specular reflexes. When the Nyquist frequency is considered, it is clear that a lidar system with a kHz sampling rate is required to obtain the full harmonic content of the signal from insect wing beats. The frequency content of wing beats is related to factors such as body mass, wing span and wing area through fundamental aerodynamic constraints (se e.g. [5]) and it is thus of high value for species classification purposes, see e.g. [6].

Resolved wing-beat modulation have previously been used to discriminate lidar signal of honeybees from the signal of the surrounding environment, see e.g. [7]. While pulsed Nd:YAG lasers with kHz-repetition rates were utilized in those cases, our research group has developed a kHz-continuous wave (CW) lidar system, relaying on cheap and small diode lasers. The system has been used in several field campaigns, aimed at insect detection. A method for reducing time-range data, obtained with kHz lidar, into relevant parameterized observations, such as wing beat frequency and size has also been developed. Examples of observed insect events from the kHz-lidar data, and their parameterized properties will be presented here.

## 2. METHODOLOGY

Figure 1 displays a schematic setup of the CW lidar system. The beam is expanded and transmitted by a refractor telescope, and the beam is terminated on a hard, preferably black, target. The light is collected using another refractor telescope. Range resolution is obtained by sharply imaging the laser beam onto a line-detector. This is achieved by arranging the planes of the laser beam, the detector, and the collection lens according to the Scheimpflug principle. It states that to achieve focus, the three planes must intersect along a common line, see upper panel of Fig. 1. For more information about the Scheimpflug setup see [3].

The specific data set utilized in this work was acquired in Brunnslov, Sweden, in the summer of 2013, using the Lund University Mobile Biosphere Observatory (LUMBO). LUMBO is a moveable research platform intended for quantitative monitoring of atmospheric fauna and it contains, among other instrumentation, a CW-lidar system. An 808-nm laser beam was transmitted into the atmosphere, above various patches of farmland and fields, by a refractor telescope and it was terminated on a treetop, 1966 m from the transmitter. Figure 1 display a map of the beam line at Brunnslov. The backscatter from the beam was imaged on a line scan camera with a sampling rate of 2 kHz. The samples were stored as image files, covering 4 second window.

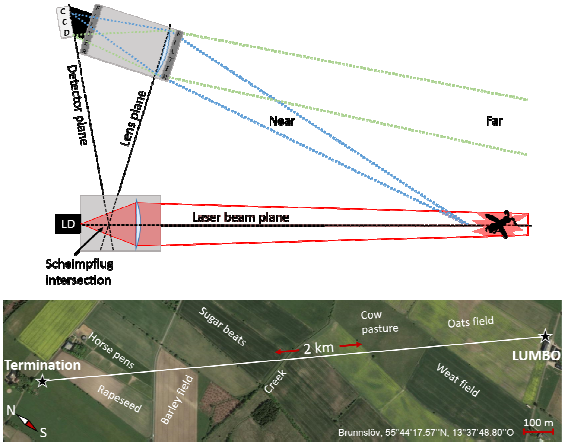


**Figure 1. Scheimpflug-lidar setup and a map of the beam line at Brunnslov.**

## 3. DATA PROCESSING

To be able to handle the analysis of the large volume of image files acquired during a measurement campaign in an efficient and robust manner, an algorithm which automatically identifies and extracts insect events from the files has been developed. The algorithm analyzes the insect events and parameterizes properties such as size and wing beat frequency. Identification and extraction of insect events from the data are done by defining OCS thresholds above the static OCS level, $\Phi_{stat}$. $\Phi_{stat}$ is the laser induced signal when no insect, or other large particle, is present in the beam, and it is a result of the laser backscattering from the beam termination and the air in the atmosphere. It is defined as the median intensity value over a 4 second time window. Each range has a specific threshold value and it is obtained by exploiting the asymmetry of the distribution in an intensity histogram over the time window (see Fig 2). When no rare events occurs in the time window the histogram has a Gaussian distribution (parabola with log scale), around $\Phi_{stat}$, where the width of the distribution represent the noise level. An insect event will cause the Gaussian distribution to become skewed towards higher values, which can be seen in Fig 2. The threshold is defined by folding the minimum OCS value over the static median value, and multiplying with a factor corresponding to the minimum signal-to-noise ratio (SNR) to be considered. Hereafter we identify rare events by considering all cases where the OCS exceeds the threshold.

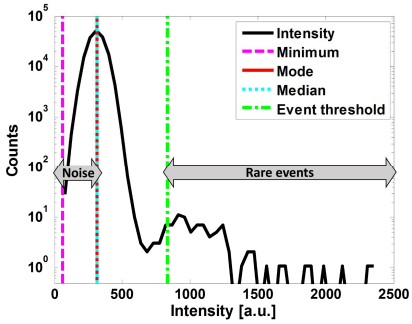


**Figure 2 Histogram of intensity values in a 4 second window. The asymmetry of the distribution, is used to define a threshold for an insect event.**

A typical lidar signal from an insect is modulated due to its wing beat cycle which makes it sparse in both time and space. Figure 3a presents two, modulated, lidar signals from insects in time range maps, extracted from the Brunnslov data. The time series, $\Phi_t$, of the insect events are displayed in Fig 3b. They consists of a non-oscillatory, DC contribution from the insect body during the transit time through the laser beam ($\Delta t$), and an oscillatory contribution resulting from the wing beat cycle. When the insect propels its wings, the projected cross section area which backscatters light changes and the detected signal is therefore modulated. This modulation is directly related to the wing beat cycle. Beside this incoherent modulation, the oscillatory signal from insects with glossy wings may also include a specular (coherent) part. Specular reflections show up as narrow spikes on the signal in the time domain as seen in Fig 3b, or as high harmonics in

the frequency domain. The algorithm determines the size of the body and the wings of the insect by evaluating their contributions to the time series.

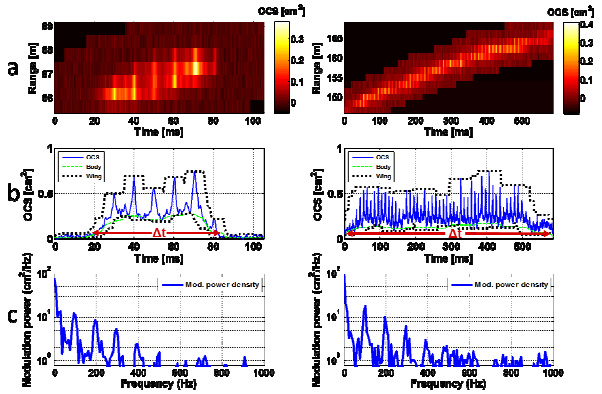


**Figure 3 a) Two insect events and b) their OCS time series, in which the contributions from the body and wings are marked. c) The power spectra of the two time series.**

The algorithm also perform frequency analysis on the time series to estimate the fundamental frequency of the wing beats, $\omega_0$. A power spectrum of $\Phi_t$ is obtained with a fast Fourier transform. The power spectra for our two case events are presented in Fig. 3c. These power spectra contains three contributions; a DC component, corresponding to the insect flying in and out of the beam, the fundamental tone of the wing beats and its harmonics, and finally noise. The power spectrum is used to make an inital guess of the fundamental frequency of the wing beats. This guess is later used to find the combination of wing beat harmonics (multiples of $\omega_0$) that best represents the original insect event. The initial fundamental tone estimation has great impact on the final parameterized $\omega_0$, and the best method to obtain a robust estimation for all events is still being developed.

The first step to find $\omega_0$ is to express the wing contribution of the event as a linear combination of harmonic basis functions, and thus acquire the absolute strength and phase of the different harmonics in the event signal. The strength and phase are then fitted on top of the harmonic functions to recreate the oscillating signal contribution for the wing beats. To determine the final $\omega_0$ and its harmonics, frequencies within 30% of the initial guess are used in the harmonic functions and the resulting signal is compared to the original event, using a least square fit. The $\omega_0$, which gives the best fit, is the fundamental wing beat frequency of the insect and this is used to obtain the final parameterized event. The parameterized fundamental frequency and harmonics obtained for the case events are represented in Fig 4. For the event in Fig 4a, the strength of $\omega_0$ is lower than the strength of $2\omega_0$. It is our understanding that this may occur when the detector sees the insect from the side, since it will appear big twice during one wing beat cycle. If the detector instead sees the insect from the back or the front it only appears large once per cycle and $\omega_0$ should dominate (as is the case for the event in Fig 4b). By this reasoning, it is probable that the insect in Fig 4a flew across the beam, while the movement of the insect in Fig 4b was more along the beam direction. This conclusion also correlates with the duration of the two events.

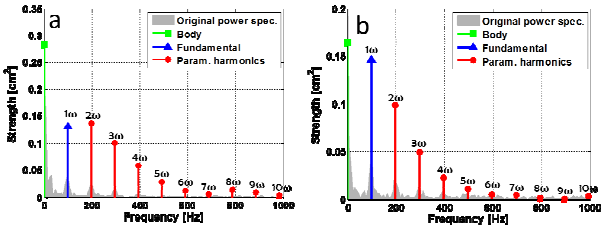


**Figure 4 The strength of the fundamental frequency and the harmonics for the two case events.**

## 4. STATISTICS

Some examples of statistical result the lidar system and data analysis method can deliver to researchers are presented below. Figure 5 displays a scatter plot of all parameterized events during one night of measurements. It shows body size, wing size, range, time and $\omega_0$ of each event. The scatterplot contains 2154 parameterized events. A majority of the insects detected close to the detector are small in size while the insects detected at longer ranges are large. This is due to a bias in the system which is a result of a higher system sensitivity closer to the detector. The best way to determine and compensated for the system sensitivity is still being investigated. Figure 6 presents a 2-D contour plots of $\omega_0$ against time of night. It is clear from both the scatter plot and the contour plot that there are two peaks in insect activity during the night. Both occurs around twilight (dawn and dusk). This is not very surprising, since many insects are crepuscular,

meaning that they are primarily active during twilight. In Fig 6, it is clear that the insects have a wide range of wing beat frequency with peaks in an interval around 100 Hz. The peaks at dusk and dawn are at roughly the same frequencies which might indicate that it is the same species (which have the same $\omega_0$) that are active at these times.

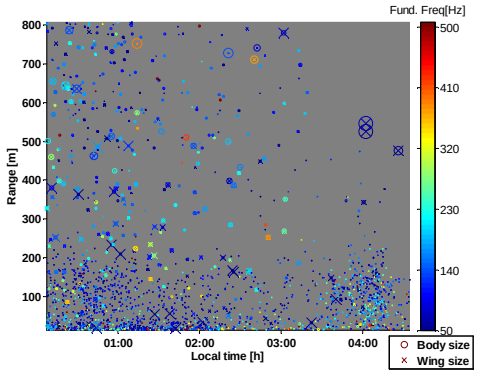


**Figure 5 Scatter plot of all the parameterized insect events during one night of measurements at Brunnslov.**

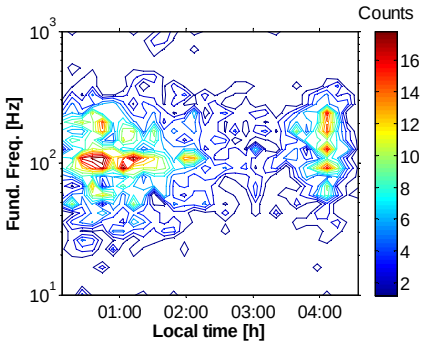


**Figure 6. 2-D contour plot of all insects during the measurements period. It displays the fundamental frequency vs time of night.**

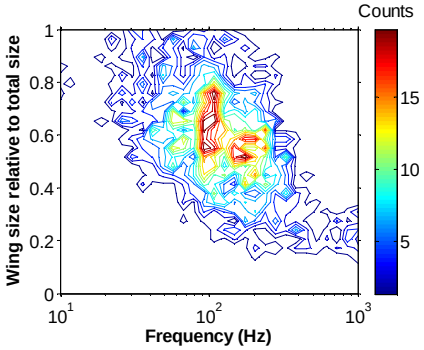


**Figure 7. 2-D contour plot of all insects during the measurement period. It displays the relative wing size vs fundamental frequency.**

Figure 7 displays a 2-D contour plot representing the wing size relative to total size and $\omega_0$ of all the parameterized insects. The distribution indicates that insects with large wings compare to their body have a low wing beat frequency and insects with small wings have a high wing beat frequency.

## 5. CONCLUSIONS

Our kHz-lidar system and data analysis routine are still being developed. Aspects, such as system sensitivity at different ranges and fundamental tone estimation must be further investigated and improved. Nevertheless, the system already displays great potential to provide entomological biologists and ecologists with extensive and time resolved data on insect activity and insect properties. Such properties can be used by the researchers for species identification and study of the behavior and movements of insects, which in turn can be used to understand spreading of insect borne diseases, pests and pollinators.

One future aim is to create a database which relates insect properties, such as wing beat frequency content, to species and possibly sex and age group. Such a tool would make it possible for us to provide ecologists with very valuable information in the form of species, age and sex distributions in time and space.

## REFERENCES


[1] Gillott, C. 2005: Entomology, 3rd Edition, Dordrecht: Springer.

[2] Kovalev, V. A., W. E. Eichinger, 2004: Elastic lidar: theory, practice, and analysis methods, John Wiley & Sons.

[3] Brydegaard, M., A. Gebru, S. Svanberg, 2014: Super resolution laser radar with blinking atmospheric particles – application to interacting flying insects, *Prog. in Electromagnetics Research*, **147**, 141-151.

[4] Sotavalta, O., 1952: Flight-Tone and Wing-Stroke Frequency of Insects and the Dynamics of Insect Flight, *Nature*, **170,** 1057-1058, 12/20/print.

[5] Fry, S. N., R. Sayaman, M. H. Dickinson, 2005: The aerodynamics of hovering flight in Drosophila, J. Exp. Biol., **208**, 2303-2318.

[6] Moore, A., R. H. Miller, 2002: Automated identification of optically sensed aphid (Homoptera: Aphidea) wingbeat waveforms, Ann. Entomol. Soc. Am. **95(1)**, 1-8.

[7] Hoffman, D. S., A. R. Nehrir, K. S., Repasky, J. A. Shaw, J. L., Carlsten, 2007: Range-resolved optical detection of honeybees by use of wing-beat modulation of scattered light for locating land mines, Appl. Opt, **46 (15)**, 3007-3012.